

Sudomotor Innervation in Transthyretin Amyloid Neuropathy: Pathology and Functional Correlates

Chi-Chao Chao, MD, PhD,¹ Cho-Min Huang, BS,² Hao-Hua Chiang, MS,²
 Kai-Ren Luo, PhD,² Hung-Wei Kan, MS,² Naomi Chu-Chiao Yang, MS,²
 Hao Chiang, PhD,² Whei-Min Lin, MS,² Shu-Mei Lai, MS,²
 Ming-Jen Lee, MD, PhD,¹ Chia-Tung Shun, MD, PhD,^{3,4} and
 Sung-Tsang Hsieh, MD, PhD^{1,2,5,6}

Objective: Autonomic neuropathy is a major component of familial amyloid polyneuropathy (FAP) due to mutated transthyretin, with sudomotor failure as a common manifestation. This study aimed to investigate the pathology and clinical significance of sudomotor denervation.

Methods: Skin biopsies were performed on the distal leg of FAP patients with a follow-up duration of 3.8 ± 1.6 years. Sudomotor innervation was stained with 2 markers: protein gene product 9.5 (PGP 9.5), a general neuronal marker, and vasoactive intestinal peptide (VIP), a sudomotor nerve functional marker, followed by quantitation according to sweat gland innervation index (SGII) for PGP 9.5 (SGIIPGP 9.5) and VIP (SGIIVIP).

Results: There were 28 patients (25 men) with Ala97Ser transthyretin and late onset (59.9 ± 6.0 years) disabling neuropathy. Autonomic symptoms were present in 22 patients (78.6%) at the time of skin biopsy. The SGIIPGP 9.5 and SGIIVIP of FAP patients were significantly lower than those of age- and gender-matched controls. The reduction of SGIIVIP was more severe than that of SGIIPGP 9.5 ($p = 0.002$). Patients with orthostatic hypotension or absent sympathetic skin response at palms were associated with lower SGIIPGP 9.5 ($p = 0.019$ and 0.002 , respectively). SGIIPGP 9.5 was negatively correlated with the disability grade at the time of skin biopsy ($p = 0.004$), and was positively correlated with the interval from the time of skin biopsy to the time of wheelchair usage ($p = 0.029$).

Interpretation: This study documented the pathological evidence of sudomotor denervation in FAP. SGIIPGP 9.5 was functionally correlated with autonomic symptoms, autonomic tests, ambulation status, and progression of disability.

ANN NEUROL 2015;78:272–283

Familial amyloid polyneuropathy (FAP) due to transthyretin (TTR) mutations is a relentless disease affecting the peripheral nervous system and vital organs.¹ There are >100 point mutations of TTR with ethnic preferences.² For example, Val30Met is the most common point mutation in Western countries and Japan,³ as is Ala97Ser in Taiwan.⁴ FAP typically results in a generalized disabling neuropathy affecting the autonomic,

sensory, and motor components of the peripheral nerve system.

Autonomic neuropathies involving various organ systems are important and can sometimes be early clinical presentations of FAP. Sudomotor failure is a major component of autonomic neuropathy.^{1,5} Most clinical evaluations of autonomic neuropathy depend on functional tests; there is, however, a lack of pathological

View this article online at wileyonlinelibrary.com. DOI: 10.1002/ana.24438

Received Jan 8, 2015, and in revised form Apr 25, 2015. Accepted for publication May 10, 2015.

Address correspondence to Dr Hsieh, Department of Neurology, National Taiwan University Hospital, 7 Chung-Shan S Road, Taipei 10002, Taiwan.
 E-mail: shsieh@ntu.edu.tw

From the ¹Department of Neurology, National Taiwan University Hospital; ²Department of Anatomy and Cell Biology, National Taiwan University College of Medicine; ³Department of Pathology, National Taiwan University Hospital; and ⁴Department of Forensic Medicine; ⁵Graduate Institute of Brain and Mind Sciences, and ⁶Graduate Institute of Clinical Medicine, National Taiwan University College of Medicine, Taipei, Taiwan

Additional supporting information can be found in the online version of this article.

examinations to demonstrate the degeneration of the peripheral autonomic nerves in FAP. Because sweat glands are located in the dermis, this anatomical position offers potential to evaluate nerve fibers innervating sweat glands via skin biopsy. We, and several groups, have developed a morphometric analysis method to quantify the pathology of sudomotor innervation from skin biopsies, that is, a sweat gland innervation index (SGII).^{6,7} Sudomotor innervation is reduced in diabetes^{7,8} and correlated with the symptoms of diabetic autonomic neuropathy.⁹ In FAP, however, the pathology of sudomotor innervation and its clinical significance remained unclear; given that autonomic dysfunction was a major symptom. Traditionally, sudomotor nerve innervation is examined with a general neuronal marker of protein gene product 9.5 (PGP 9.5).^{6,7} A further critical issue is whether there exists sudomotor innervation of different phenotypes showing different innervation patterns, for example, vasoactive intestinal peptide (VIP).¹⁰

This study aimed to investigate the pathology of sweat gland innervation in FAP of TTR Ala97Ser by analyzing the phenotypes of sweat gland innervation with 2 different markers: a general neuronal marker PGP 9.5, and a sudomotor nerve marker VIP. Specifically, we examined the clinical significance of the sudomotor degeneration in relation to (1) neurological symptoms, (2) autonomic functional tests, and (3) functional deficits of disability grade.

Subjects and Methods

Participants

Patients with TTR Ala97Ser mutation and polyneuropathy were identified from the database of the Department of Neurology, National Taiwan University Hospital, Taipei, Taiwan from January 1, 2000 to December 31, 2013. Patients were regularly followed at our hospital, and clinical information including all relevant examinations was retrieved. All had received complete workup for the diagnosis of polyneuropathy including physical and neurological examinations, laboratory tests, nerve conduction studies, quantitative sensory testing, autonomic function tests, and skin biopsy. The inclusion criteria consisted of: (1) length-dependent neuropathy with clinical evidence of limb weakness and sensory symptoms, (2) electrophysiological evidence of axonal polyneuropathy on nerve conduction studies, and (3) TTR Ala97Ser mutation. Patients with concomitant systemic diseases were excluded from further analyses. Exclusion criteria included diabetes mellitus, chronic kidney disease, syphilis, human immunodeficiency virus infection, autoimmune diseases, malignancies, history of using neurotoxic medications, alcoholism, or toxin exposure as determined by detailed history and the results of relevant laboratory tests including hematological, biochemical, endocrine, infection, malignancy, nutritional, and autoimmune profiles. After enrollment, clinical and

laboratory data were retrieved for further analysis. The disability was evaluated according to the polyneuropathy disability score on a scale of 1 to 4: grade 1, sensory symptoms without motor disturbances; grade 2, minor motor disturbances and ability to walk without aids; grade 3, major motor disturbances and requiring support to walk; grade 4, confinement to a bed or a wheelchair.¹¹

For comparison of sweat gland innervation with the FAP group, age- and gender-matched subjects were retrieved from our database. Skin biopsy was performed after informed consent was obtained from the patients. The protocol was approved by the Ethics Committee of National Taiwan University Hospital, Taipei, Taiwan.

Nerve Conduction Studies

Nerve conduction studies were performed with a Nicolet (Madison, WI) Viking IV Electromyographer on all patients as per standardized methods.¹² The amplitude of the sural sensory action potentials (SAP) and the amplitude of the compound muscle action potentials (CMAPs) on distal stimulation from the peroneal nerve were analyzed.

Quantitative Sensory Testing

Quantitative sensory testing was performed to measure the sensory thresholds of warm/cold and vibratory sensations with a Thermal Sensory Analyzer and a Vibratory Sensory Analyzer (Medoc Advanced Medical System, Minneapolis, MN), respectively. These procedures have been detailed previously.^{13,14} The level method was the algorithm used to measure thermal thresholds. The skin of the foot dorsum was the test site. Thermal thresholds were expressed as warm threshold temperature and cold threshold temperature. Vibratory thresholds were measured with similar algorithms at the lateral malleolus, and were expressed in micrometers. These measured thresholds were compared with normative values for age.

Autonomic Function Tests

R-R interval variability (RRIV) for the cardiac-vagal function and sympathetic skin response (SSR) for the sudomotor function were performed using established protocols on the Nicolet Viking IV Electromyographer.¹⁵ The RRIV was obtained during rest position and forced deep breathing. Each test was repeated 3 times, and the mean value was compared with that for the age-matched controls in our laboratory. SSR was recorded in the palm and sole, and the results were interpreted as present or absent, but were not evaluated quantitatively because of variations in the latencies and the amplitudes of SSR.

Skin Biopsy

Skin biopsy was performed by following established procedures after informed consent had been obtained.^{16,17} A 3mm diameter skin punch was taken from the distal leg 10cm proximal to the lateral malleolus under local anesthesia with 2% lidocaine. All patients tolerated the procedure with no obvious discomfort.

In the present study, the skin biopsy of all patients were performed between 2000 and 2010 (median year = 2007).

Immunohistochemistry of Sweat Gland and Epidermal Innervation with PGP 9.5

Skin sections were immunostained with PGP 9.5 to demonstrate nerve fibers, and then counterstained with Congo red to reveal sweat glands as described previously.⁹ In brief, the sampled skin tissue was fixed overnight in 2% paraformaldehyde-lysine-periodate. Sections of 50 μ m perpendicular to the dermis were immunostained with rabbit antiserum to PGP 9.5 (1:1,000; UltraClone, Isle of Wight, UK). Biotinylated goat antirabbit immunoglobulin G (Vector Laboratories, Burlingame, CA) and the avidin-biotin complex (Vector Laboratories) were sequentially applied. The reaction product was demonstrated with chromogen SG (Vector Laboratories). The sections were termed "conventional sections." Additional conventional sections were further counterstained with 1% Congo red (Muto Pure Chemicals, Tokyo, Japan) for 5 minutes to reveal the territory of the sweat gland. Sections were dehydrated with anhydrous alcohol and mounted using DPX (Sigma, St Louis, MO), a nonaqueous synthetic resin. Congo red staining showed well-defined areas of sweat glands and thus facilitated measurements of sweat gland area.⁶ We quantified the epidermal innervations on conventional sections and the sweat gland innervation on the Congo red-counterstained sections.

To understand the nature of Congo red staining in sweat glands, we observed sections under polarized microscopy. Because some of these patients received sural nerve biopsy for diagnostic purpose, we retrieved 3 sural nerve biopsies of FAP for comparison.

Quantitation of Sweat Gland Innervation by PGP 9.5 Immunohistochemistry and Congo Red

All identifying information on the slides was masked before quantification. Sections were observed under a $\times 20$ objective on a DM2500 light microscope (Leica Microsystems, Wetzlar, Germany) equipped with a DFC490 charge-coupled device (Leica Microsystems). The acquired image was then opened with Photoshop CS3 (Adobe Systems, San Jose, CA) to quantitate sweat gland innervation. The areas of PGP 9.5⁺ nerve fibers and Congo red-stained sweat glands were measured on each section. We designated SGII of the selected sweat gland according to the formula: $SGII = \text{nerve fiber area} / \text{sweat gland area} \times 100\%$, which represented the area of nerve fibers normalized to the area of the sweat gland according to our previous report of quantifying sweat gland innervations.⁹ The mean of all SGIIs (3–7 sweat glands from 3 different sections for each subject) was defined as the SGII of a given subject. The normative values of SGII based on PGP 9.5 staining (SGIIPGP 9.5; mean \pm standard deviation [SD], 5th percentile) from our laboratory were 4.33% \pm 1.32%, 2.36% for males and 5.33% \pm 1.41%, 2.69% for females.⁹ SGIIPGP 9.5 was classified as abnormal if SGIIPGP 9.5 was $< 2.36\%$ and $< 2.69\%$ for males and females, respectively.

Immunohistochemistry and Quantitation of Sweat Gland Innervation with VIP

For demonstrating sweat glands and functional markers of sudomotor nerves, additional sections were stained with double immunofluorescence: Na-K-Cl cotransporter (NKCC1) for sweat gland cells, and VIP for sudomotor nerves. Sections were incubated with mouse NKCC1 antiserum (clone T4, 1:500; Developmental Studies Hybridoma Bank, Iowa City, IA) and rabbit VIP antiserum (1:100; ImmunoStar, Hudson, WI) overnight. Signals of NKCC1 and VIP were visualized with Cy3 (1:100; Jackson ImmunoResearch, West Grove, PA) and fluorescein isothiocyanate (FITC; 1:100, Vector Laboratories), respectively. After rinsing, sections were mounted with 2% n-propyl gallate in 60% glycerol. The immunofluorescent sections were observed under a $\times 20$ objective (with oil) on a confocal microscope (TCS SP5, Leica Microsystems). The Cy3 signals (for sweat glands) and FITC signals (for nerve fibers) were imaged after excitation with a HeNe543 laser and an argon488 laser, respectively. The images were obtained through z-section stacking, which overlapped a series of phases scanned along the z-axis of the skin section. The acquired images were merged for colocalization of the sweat glands and their surrounding nerve fibers on skin sections. At least 3 qualified sweat glands from all skin sections were used for the quantitative analysis of a given subject as in our previous report.⁶

The acquired images were opened in Photoshop CS3. On each section, the areas of sweat glands (in red) and the nerve fibers (in green) were measured separately. For measuring sweat gland areas, the "select/color range" command (the magic wand tool) was used (under the red channel), which determined the margins of sweat glands automatically without manual tracing by the operator. The sum of pixel values of the selected areas represented the sweat gland areas. Under the green channel, the same "select/color range" command was applied to measure the area of surrounding nerve fibers. The selected pixel values represented the nerve fiber areas. The derived SGII was the nerve fiber area normalized by the sweat gland area (as a percentage) for the given sweat gland. The mean of all SGIIs was defined as the SGII of VIP (SGIIVIP) for a given subject as described in SGIIPGP 9.5.⁶ The normative values of SGIIVIP (mean \pm SD, 5th percentile) from our laboratory were 3.17% \pm 2.38%, 0.95% for males, and 5.52% \pm 3.67%, 1.04% for females. SGIIVIP was classified as abnormal if SGIIVIP was $< 0.95\%$ and $< 1.04\%$ for males and females, respectively.

Quantification of Epidermal Innervation

Epidermal innervation was quantified from the conventional sections according to established criteria in a coded fashion with the examiners blinded to the clinical information. PGP 9.5-immunoreactive nerve fibers in the epidermis of each section were counted at a magnification of $\times 40$ with an BX40 microscope (Olympus, Tokyo, Japan) through the depth of the entire section. Intraepidermal nerve fiber (IENF) density was therefore derived and expressed as the number of fibers/mm of the epidermal length. In the distal leg, normative values from our laboratory (mean \pm SD, 5th percentile) for IENF were

11.16 ± 3.70, 5.88 fibers/mm for subjects aged <60 years and 7.64 ± 3.08, 2.50 fibers/mm for subjects aged ≥60 years.¹⁸ The cutoff point of IENF density was 5.88 and 2.50 fibers/mm in these 2 age groups, respectively.

Immunohistochemistry of TTR

To examine whether amyloid was on the skin biopsies and to test whether amyloid was related to TTR, we performed TTR immunohistochemistry on skin and sural nerve biopsies following the same protocols described in the preceding sections with modifications; that is, anti-TTR antiserum (1:500; Dako, Glostrup, Denmark) and chromogen 3,3'-diaminobenzidine (Sigma) were used.

Statistical Analysis

Numerical variables were expressed as the mean ± SD, and were compared with *t* tests if the data followed a Gaussian distribution. If the sample size was small, the numerical variables were compared using a nonparametric test (Wilcoxon rank sum test). Fisher exact test was used to compare categorical data. Correlations between variables were graphically analyzed using Stata (StataCorp, College Station, TX) and Prism (GraphPad Software, San Diego, CA). For analysis of the degree of sudomotor innervation, SGIIPGP 9.5 and SGIIVIP of each patient were converted to a percentile rank as an additional parameter according to the normative data of SGIIPGP 9.5 and SGIIVIP, respectively. Results were considered significant at *p* < 0.05.

Results

Clinical Presentations

There were 28 patients (25 men, Supplementary Table) with genetic confirmation of the Ala97Ser mutation in the *TTR* gene, and all had clinical and electrophysiological evidence of polyneuropathy. The onset of neuropathic symptoms was at the age of 59.9 ± 6.0 (range = 48–71) years. The duration between the onset of neuropathic symptoms and the clinical evaluation with skin biopsy was 2.3 ± 1.2 (range = 1–5) years. At the time of skin biopsy, autonomic symptoms were present in 22 patients (78.6%), and included gastrointestinal, cardiovascular, genitourinary, and sweating dysfunctions. All patients had difficulties in ambulation: grade II (21), grade III (6), and grade IV (1). Paresthesia was present in all patients, with 15 of them (53.6%) having neuropathic pain. Sensations of large and small fibers were impaired. During the follow-up (3.8 ± 1.6 years after skin biopsies), all patients had a progressive course leading to disability, with the interval from symptom onset to the time with a grade IV (wheelchair usage) disability being 4.4 ± 1.6 (range = 2–8) years.

Electrophysiological Studies

To understand the global physiological picture of FAP, we conducted autonomic function tests (SSR and RRIV) and

nerve conduction studies. SSR was absent in the palms of 9 patients (32.1%), and in the soles of 22 patients (78.6%). Except for 3 patients with arrhythmia during the tests, RRIV was reduced at rest and during deep breathing in 22 patients (88%). In total, 25 patients (89.3%) had abnormalities in at least 1 autonomic functional test at the time of clinical evaluation. Nerve conduction studies showed sensorimotor polyneuropathy of axonal degeneration pattern in all patients. Quantitative sensory testing showed elevated thermal thresholds in 24 patients and elevated vibratory thresholds in all patients, indicating impaired sensory functions of both large and small sensory nerves.

TTR Amyloid Detection in Skin and Nerve Biopsies

In the Congo red–stained sections under polarized light microscopy, typical amyloids in the vascular wall of an endoneurial arteriole on sural nerve biopsies showed apple-green birefringence (Fig 1A, B). In contrast, sweat glands on skin sections did not reveal such a pathognomic pattern of amyloids. In the skin biopsies of all patients, we only detected Congo red⁺ materials in the arteriole of a small dermal nerve bundle with yellow birefringence from 1 patient (see Fig 1C–F). Congo red binds the secondary structures of a variety of chemicals, including amyloids of TTR or amyloid precursor protein,¹⁹ variable native proteins,²⁰ and lipopolysaccharides in bacteria *Shigella*.²¹ Some of these complexes exhibit dichromatic spectrum under polarized microscopy depending on their chemical natures, for example, apple-green birefringence in amyloids.^{20,22} In this study, the pattern of Congo red staining in sweat glands was different from that of amyloids; that is, amyloids in small arterioles of sural nerve biopsies showed typical apple-green birefringence, which was absent in Congo red–stained sweat glands of skin biopsies.

We further examined whether amyloid was related to TTR by immunohistochemistry with anti-TTR antibody. TTR immunoreactivity was documented in the amyloids surrounding endoneurial arterioles in sural nerve biopsies (Fig 2A, B), confirming the nature of TTR-related amyloids. Skin sections from the patient described in Figure 1E and F were further stained with PGP 9.5, TTR, and Congo red (see Fig 2C–F). There were scanty PGP 9.5⁺ periglandular nerve fibers and fragmented nerve fibers in dermal nerve bundles. The Congo red counterstaining in sweat glands exhibited red autofluorescence. There was no TTR immunoreactivity in Congo red–stained sweat glands. Thus specific TTR immunoreactivity was not detected in the skin of FAP patients. These findings demonstrated that the pathogenic roles of TTR in amyloids and Congo red–stained sweat glands were independent of TTR. The absence of specific TTR

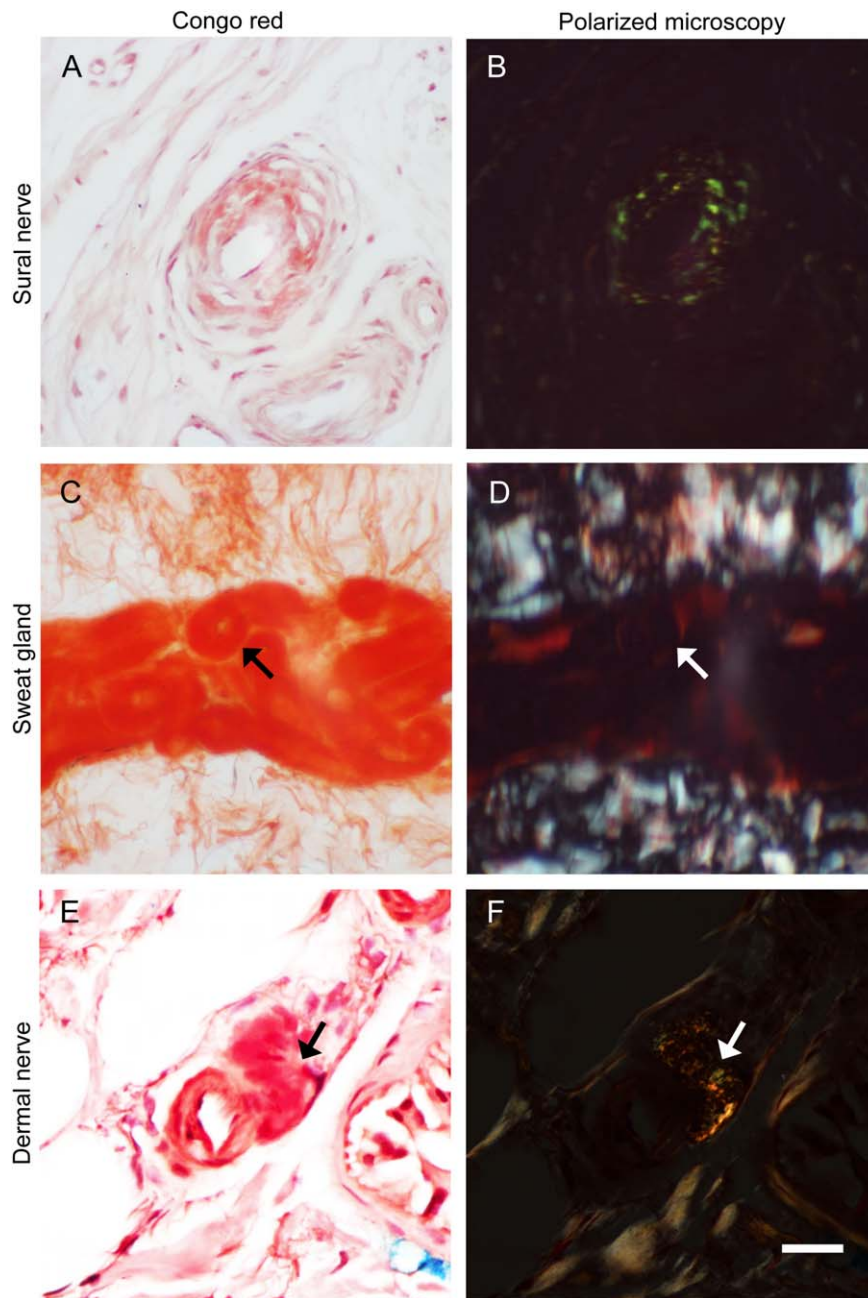


FIGURE 1: Congo red staining and polarized microscopic examinations of sural nerve and skin biopsies from patients with familial amyloid polyneuropathy (FAP). Sections of sural nerve (A, B) and skin (C–F) biopsies were stained with Congo red (A, C, and E) and observed under a polarized microscope (B, D, and F). (A, B) Congo red–stained materials in an arteriole of the sural nerve exhibited apple-green birefringence under polarized microscopy. (C, D) Secretory coils of sweat glands were stained with Congo red (*arrow*) but did not show birefringence under polarized microscopy. (E, F) In a dermal nerve bundle from an FAP patient, Congo red⁺ materials were detected surrounding a small arteriole (*arrow*), which showed birefringence under polarized microscopy. Scale bar = 50 μ m for A and B, 200 μ m for C and D, and 25 μ m for E and F.

immunoreactivity in skin biopsies may reflect a very low prevalence of amyloids in the skin of FAP.

Sweat Gland and Epidermal Innervation Based on PGP 9.5 Staining

To investigate the pathology of sweat gland innervation, we first examined this issue by staining skin biopsies with

PGP 9.5 according to conventional methods.²³ In the dermis of the control skin, PGP 9.5⁺ nerve fibers appeared as a dense and linear pattern circling the sweat glands, which had mild staining intensity higher than the background and much lower than the staining intensity of nerve fibers as described before.^{6,7} In the skin of FAP patients, the PGP 9.5⁺ nerve fibers surrounding sweat glands were markedly decreased (Fig 3A, B).

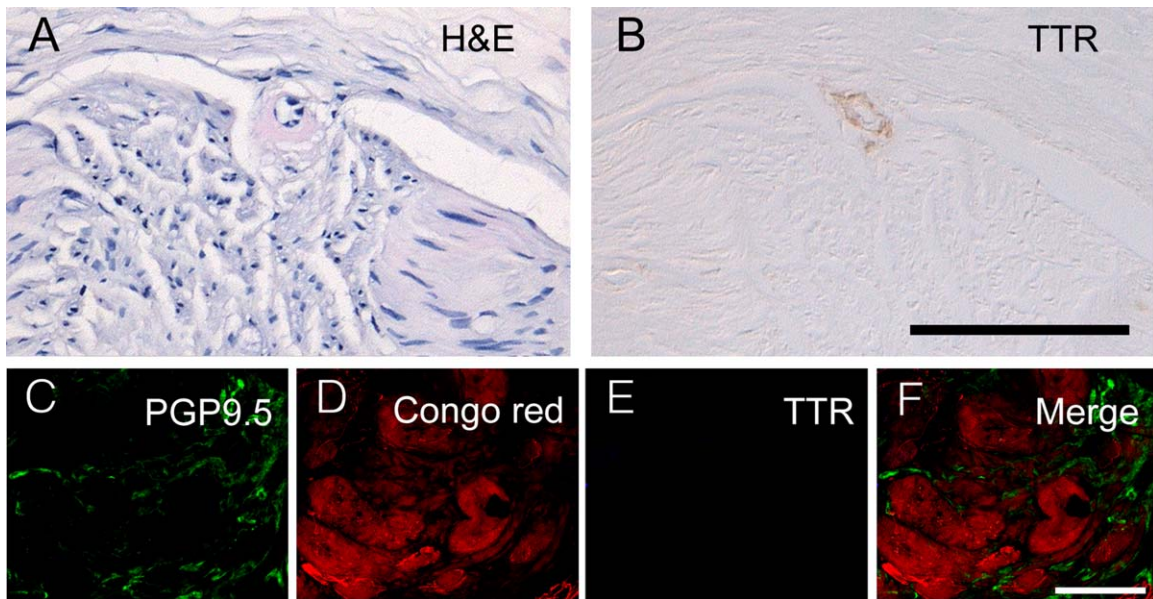


FIGURE 2: Transthyretin (TTR) expression in sural nerve and skin biopsies in familial amyloid polyneuropathy (FAP). Sections of sural nerves (A, B) were stained with hematoxylin and eosin (H&E; A) and immunohistochemistry of TTR (B), respectively. Immunofluorescent staining with protein gene product 9.5 (PGP 9.5; labeled with green fluorescence in C) and TTR (labeled with blue fluorescence in E) followed with Congo red counterstaining (with red autofluorescence in D) was performed on the skin biopsy from the same FAP patient in Figure 1C to F. (A, B) There was TTR immunoreactivity in amyloid with eosinophilic amorphous appearance surrounding an arteriole from sural nerve biopsy. (C–F) Scanty PGP 9.5⁺ nerve fibers were detected surrounding sweat glands, which exhibited red autofluorescence after Congo red staining. In these Congo red–stained sweat glands, there was no TTR immunoreactivity. Scale bar = 100 μ m in B applied to A and B, 50 μ m in F applied to C–F.

In the epidermis of the control skin, there were distinct varicose IENFs and subepidermal nerve plexuses appearing as dense nerve bundles. In the epidermis of the FAP skin, nearly all IENFs were depleted, and nerve fibers with a fragmented profile in the dermal nerve bundles were observed (see Fig 3C, D).

To make the sweat glands clear for quantifying sweat gland area as the denominator of SGII, we performed PGP 9.5 immunohistochemistry and counterstained with Congo red for sweat glands.⁹ In the dermis of the control skin, sweat glands appeared as red coils and sudomotor nerves were demonstrated with dense PGP 9.5⁺ fibers forming linear and varicose patterns circling the secretory coils of sweat glands (Fig 4A). These patterns represented nerve trunks and the terminal parts of sudomotor nerves. In FAP patients, there was significant reduction of nerve fibers innervating sweat glands and only a small portion of the entire sweat glands was surrounded by nerve fibers, indicating nerve degeneration (see Fig 4B).

Sweat Gland Innervation Based on VIP-NKCC1 Staining

To further examine the changes in the phenotypic patterns of sweat gland innervation, we performed immunofluorescence staining of skin biopsies with VIP for sudomotor nerve fibers, and NKCC1, a transporter

protein located in sweat gland cells, for sweat glands.²⁴ In the dermis of the control skin, the sweat glands appeared as red tubular structures surrounded by VIP⁺ sudomotor nerve fibers with dense linear and circular patterns (Fig 5A–C). In FAP patients, only scanty VIP⁺ sudomotor nerve fibers with fragmented and dotted patterns innervating sweat glands were seen, indicating sudomotor degeneration (see Fig 5D–F).

Quantitative Analysis of Sudomotor and Skin Innervation in FAP

To quantitatively analyze the above observations, we compared the innervation of sweat glands and epidermis of FAP patients with age- and gender-matched controls (Fig 6 and Supplementary Table). The SGIIPGP 9.5 in the FAP group was significantly lower than that in the control group ($1.85\% \pm 1.05\%$ vs $4.67\% \pm 1.31\%$, $p < 0.001$), and 18 patients (64.3%) had reduced SGIIPGP 9.5. The SGIIVIP in the FAP group was also significantly lower than that in the control group ($0.11\% \pm 0.16\%$ vs $3.84\% \pm 2.48\%$, $p < 0.001$). SGIIVIP was reduced in all patients (100%), indicating that the frequency of sudomotor denervation was higher in VIP than in PGP 9.5. We further explored the degree of sudomotor denervation by analyzing the percentile rank of SGII in the normative database between VIP⁺ and PGP 9.5⁺ nerves. The depletion of VIP⁺ sudomotor

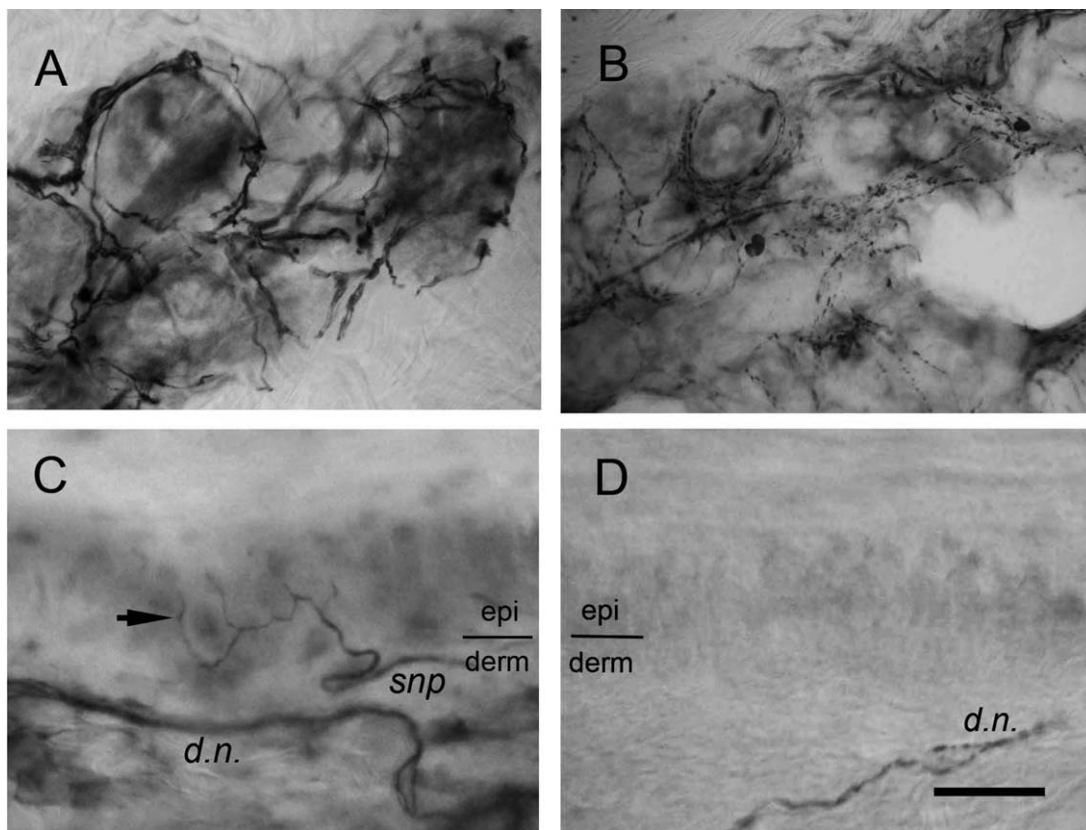


FIGURE 3: Sweat gland and skin innervation in familial amyloid polyneuropathy (FAP) due to transthyretin Ala97Ser mutation. Skin sections from control subjects (A and C) and patients with FAP (B and D) were immunostained with protein gene product 9.5. (A) In the control skin, the sudomotor nerve fibers appeared as dense immunoreactivities with a circular pattern surrounding the secretory coils of sweat glands. (B) The nerve fibers surrounding sweat glands in FAP patients were markedly reduced, and only some loose and fragmented immunoreactivities could be observed. (C) In the control skin, intraepidermal nerve fibers (arrow) with a varicose appearance ascended from the subepidermal nerve plexus (snp) at the border of the epidermis (epi) and dermis (derm). Dermal nerve fascicles (d.n.) exhibited a pattern of linear and dense immunoreactivities in the deep dermis. (D) Intraepidermal nerve fibers disappeared in the skin of FAP patients and dermal nerves became fragmented, indicating nerve degeneration. Scale bar = 45 μ m for A and B, 20 μ m for C and D.

nerves was more extensive than that of PGP 9.5⁺ sudomotor nerves (0.1 ± 0.5 percentile vs 6.3 ± 9.8 percentile, $p = 0.002$). There was no correlation between SGIIPGP 9.5 and SGIIVIP ($p = 0.971$).

The IENF density of FAP patients was markedly reduced compared to that of the control subjects (1.11 ± 1.32 vs 8.07 ± 2.83 fibers/mm, $p < 0.001$; see Fig 6C), and the IENF density was reduced in 26 patients (92.9%).

Clinical Significance of Sweat Gland Innervation

To understand the clinical significance of sweat gland innervation, we explored the relationship of sweat gland innervation with clinical parameters: (1) autonomic symptoms and functional tests (Fig 7A, B) and (2) disability grade (see Fig 7C, D). Among autonomic symptoms, the SGIIPGP 9.5 was reduced in patients with orthostatic hypotension compared to those without orthostatic hypotension ($1.33\% \pm 0.97\%$ vs $2.25\% \pm 0.95\%$, $p = 0.019$).

For autonomic functional tests, SGIIPGP 9.5 was related to the SSR at the palm: lower in patients with absent SSR at the palm than in those with present SSR at the palm ($1.03\% \pm 0.68\%$ vs $2.25\% \pm 0.97\%$, $p = 0.002$). Furthermore, the SGIIPGP 9.5 was negatively correlated with the disability grade at the time of skin biopsy ($r = -1.03$, $p = 0.004$), and was positively correlated with the interval from the time of skin biopsy to the time of wheelchair usage ($r = 0.33$, $p = 0.029$), indicating that a lower SGIIPGP 9.5 was associated with higher disability grade at the time of skin biopsy and more rapid progression of disability during follow-up. There was no correlation of SGIIVIP with autonomic symptoms, the disability at the time of skin biopsy, or the progression of disability. We also explored the relationship of the IENF density and parameters of nerve conduction studies with these disability indexes. The IENF density and the SAP of sural nerves had no correlation with the disability grade at skin biopsy or further

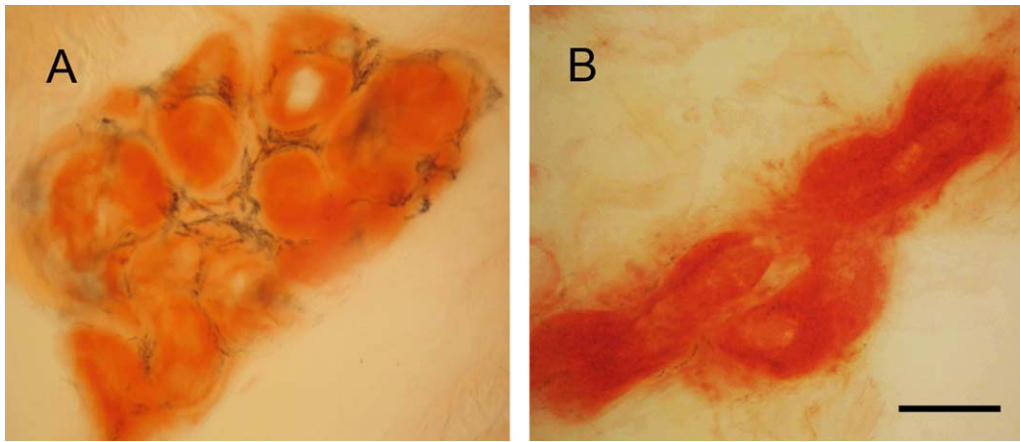


FIGURE 4: Sweat gland innervations in familial amyloid polyneuropathy (FAP). Skin sections were immunostained with protein gene product 9.5 (PGP 9.5) antiserum and then counterstained with Congo red. (A) In the control skin, sweat glands appeared as red coils and were surrounded by the linear and varicose sudomotor nerve fibers of dense PGP 9.5 immunoreactivities. (B) The sweat gland innervation was markedly reduced in FAP, and only some scattered and fragmented immunoreactivities surrounding a small portion of the sweat gland could be observed, indicating sudomotor nerve degeneration. Scale bar = 50 μ m.

progression of the disability grade. The CMAP amplitude of peroneal nerve was negatively correlated with the disability grade at the time of skin biopsy ($r = -0.65$, $p = 0.004$), and was positively correlated with the interval from the time of skin biopsy to the time of wheelchair usage ($r = 0.28$, $p = 0.002$).

Discussion

The study applied 2 different makers, PGP 9.5 and VIP, to demonstrate the pathologic evidence of sudomotor denervation in FAP and the clinical significance related to autonomic symptoms and autonomic functional tests. Furthermore, the degree of sweat gland innervation by

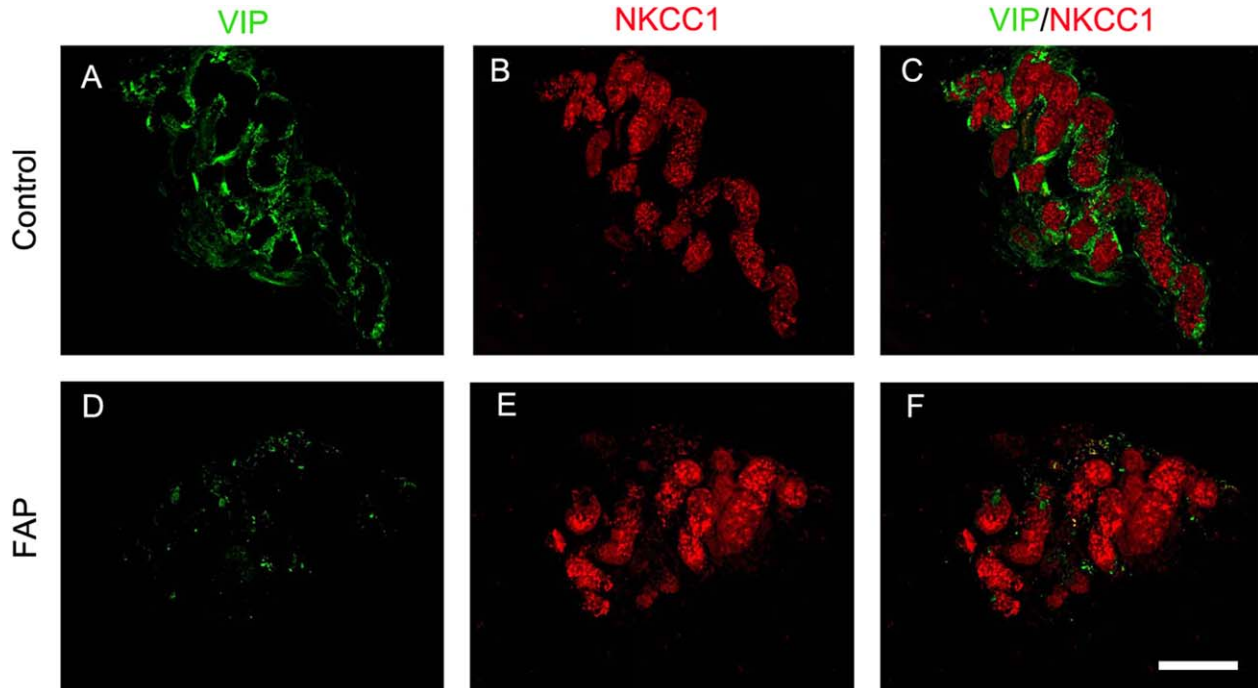


FIGURE 5: Sweat gland innervations in familial amyloid polyneuropathy (FAP). Skin sections were immunostained with vasoactive intestinal peptide (VIP; green) for sudomotor nerves (A and D), and Na-K-Cl cotransporter (NKCC1, red) for sweat glands (B and E). (A–C) In the control skin, the sudomotor nerve fibers were labeled by VIP immunoreactivities with linear and circular patterns (A) and the sweat gland was labeled by NKCC1 immunoreactivities as red coils (B). The sudomotor nerve fibers encircled the secretory coils of the sweat gland (C). (D–F) In FAP patients, the innervation of sweat glands by VIP⁺ nerves (D) surrounding NKCC1⁺ sweat glands (E) was significantly reduced. Only scattered VIP immunoreactivities surrounded the secretory coils of the sweat gland (F). Scale bar = 100 μ m.

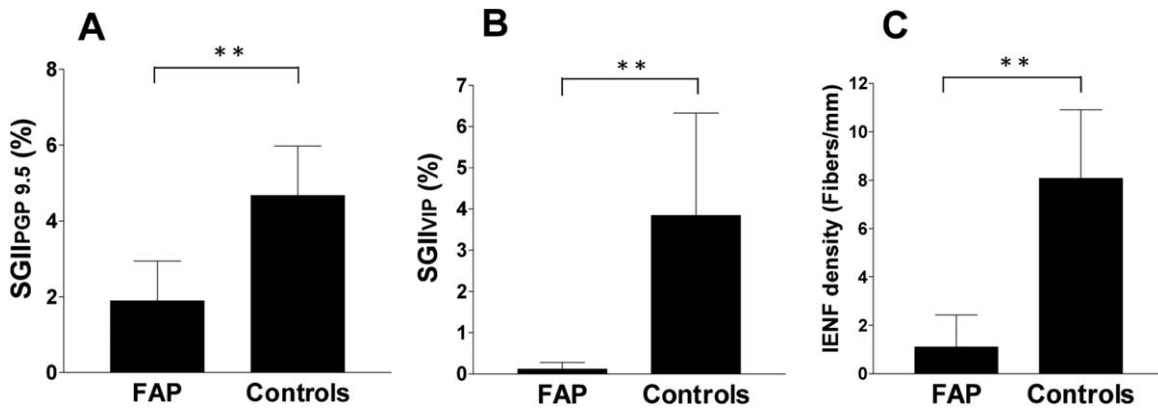


FIGURE 6: Quantitation of sweat gland and skin innervation in familial amyloid polyneuropathy (FAP). Quantitative data of sweat gland and skin innervation were analyzed according to: (A) the sweat gland innervation index by protein gene product 9.5 immunostaining (SGIIPGP 9.5), (B) the sweat gland innervation index by vasoactive intestinal peptide immunostaining (SGIIVIP), and (C) the intraepidermal nerve fiber (IENF) density. All 3 parameters were significantly reduced in the FAP group compared to the age- and gender-matched control subjects. ** $p < 0.005$.

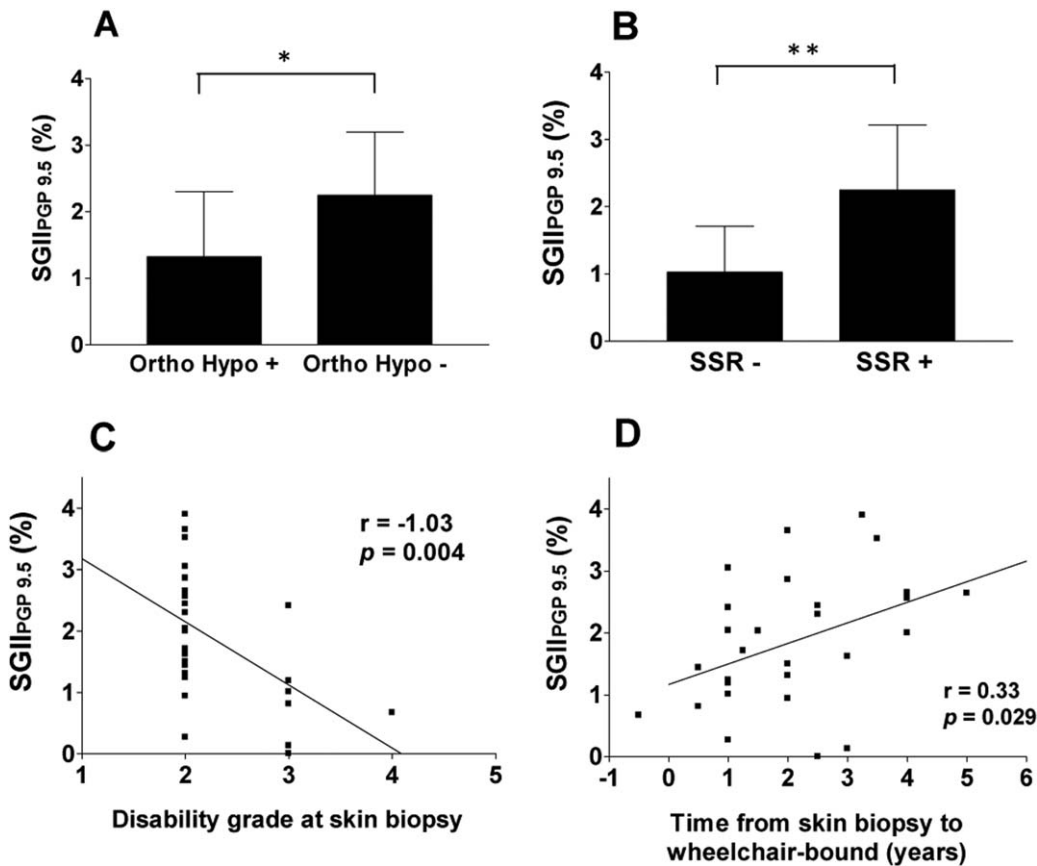


FIGURE 7: The clinical significance of sudomotor innervation in familial amyloid polyneuropathy. (A) The comparison of sudomotor innervation was made between patients with and without orthostatic hypotension. The sweat gland innervation index by protein gene product 9.5 immunostaining (SGIIPGP 9.5) was lower in patients with orthostatic hypotension (Ortho Hypo) than those without this symptom. (B) The SGIIPGP 9.5 was lower in patients with absent sympathetic skin response at the palm than in those with present response, reflecting the relationship between the pathology and functional consequence of sudomotor denervation. (C, D) SGIIPGP 9.5 was negatively correlated with the disability grade at the time of skin biopsy (C) and positively correlated with the time from skin biopsy to loss of ambulation ability (D), indicating the lower sudomotor innervation, the higher grade, and the more rapid progression of disability. SSR = sympathetic skin response at palm; + = presence; - = absence. * $p < 0.05$, ** $p < 0.005$.

PGP 9.5⁺ nerves serves as a prognostic factor for the progression of the disability grade, suggesting that combining SGII and IENF density, skin biopsy provides a new window to evaluate the general conditions of FAP.

Pathologic Evidence of Sweat Gland Denervation

The current report documents quantitative evidence of sudomotor nerve degeneration in FAP, that is, reduced SGIIPGP 9.5 and SGIIVIP, which corroborate the functional impairment of SSR. Previous investigations of autonomic failure in FAP heavily depended on functional evaluations or image studies. For example, SSR was abnormal in FAP due to Val30Met mutation.^{25,26} Combined examinations using capsule polyhydrography and computer analysis of the cardiographic R-R intervals indicated the early involvement of peripheral autonomic functions in the Val30Met variant.²⁷ Iodine-123 metaiodobenzylguanidine (MIBG) scintigraphy revealed reduced myocardial uptake in FAP, suggesting myocardial sympathetic denervation.^{28,29} However, there was limited pathologic evidence demonstrating the denervation of autonomic targets, such as a report on postmortem tissues, which showed amyloid depositions and neuronal cell loss in sympathetic ganglia with microscopic resolution.^{2,30} Sweat gland innervation was reduced in type 2 diabetic neuropathy,^{6,7,9} and we have documented that this reduction of SGIIPGP 9.5 was attributed to sudomotor nerve degeneration as demonstrated at the ultrastructural level.⁶ The current report is the first to provide direct pathologic evidence of sudomotor denervation in FAP. Taken together, these studies indicate that sudomotor denervation index was sensitive in documenting pathologic evidence of autonomic neuropathy regardless of underlying etiologies and thus is not specific for FAP. In addition to our previous demonstration of reduced IENFs as a major pathological finding on skin biopsy in the Ala97Ser variant of FAP,⁴ the present study further provides complementary evidence of sudomotor nerve degeneration on skin biopsies.

Phenotypic Difference in Sweat Gland Denervation

This study provides 2 markers of sweat gland innervation to explore the clinical significance of sweat gland innervation phenotypes. Both PGP 9.5⁺ and VIP⁺ sudomotor nerves were significantly reduced in FAP patients compared to the age- and gender-matched controls, with a difference in the abnormal rate of each examination; the frequency of reduced SGIIVIP was higher than that of reduced SGIIPGP 9.5 (100% vs 64.3%). PGP 9.5 is a general marker of neurons and peripheral nerve

fibers.^{17,31} The reduction of PGP 9.5⁺ sudomotor nerves reflects sudomotor nerve degeneration as shown at the electron microscopic level.⁶ This suggests that PGP 9.5 may serve as a structural marker of sudomotor nerves and VIP serves as a functional marker of sudomotor nerves because of its coexistence with cholinergic sympathetic innervation^{10,32} and modulation of cholinergic responses of sweat glands.^{33,34} The marked reduction of VIP⁺ nerves compared to moderate reduction of PGP 9.5⁺ nerves in sweat glands in FAP suggests that a decrease in such neuropeptide expression is far more prevalent than the overt structural degeneration of sudomotor nerves.⁸ This observation implies that a loss of functional marker was earlier than a loss of structural marker. Such a difference may be in concordance with a previous study on a mouse model of cisplatin neuropathy that found decrease in VIP⁺ nerves at an early stage followed by PGP 9.5⁺ nerve degeneration at a later stage.³⁵ Multiple mechanisms underlie such a time window in the denervation of PGP 9.5⁺ and VIP⁺ sudomotor nerves, including decreased synthesis or impaired axonal transport of neuropeptide at the early stage of FAP and progressive axonal degeneration as the disease burden increases.³⁶ Furthermore, this observation raises the possibility of testing whether such alterations of functional marker VIP at the early stage are reversible as new therapeutic clinical trials for FAP are initiated.³⁷⁻³⁹

Clinical Significance of Sudomotor Innervation Index

The sudomotor innervation index provides 2 lines of clinical information: (1) autonomic dysfunctions and (2) disability and progression of FAP. In the present study, we used SSR testing as a surrogate marker of sweat gland functions. The correlation between the SGIIPGP 9.5 and the SSR at palms suggests that SGIIPGP 9.5 may underlie the structural basis of sudomotor dysfunctions. This observation extends the previous findings in patients of diabetic neuropathy that the sudomotor innervation was concordant with symptoms of reduced sweat production.^{7,9} Future studies applying quantitative sudomotor testing such as quantitative sudomotor axon reflex test, quantitative direct and indirect reflex testing of sudomotor function, or dynamic sweat test may offer comprehensive functional analysis with structural parameters of SGII.⁴⁰⁻⁴² Orthostatic hypotension is a common cardiovascular manifestation of autonomic dysfunctions in FAP² and results from impaired baroreflex and cardiac dysfunctions.^{43,44} FAP patients with orthostatic hypotension had low basal plasma norepinephrine levels, which did not increase after postural change.⁴⁵ Pathological and imaging studies showed neuronal cell loss in sympathetic

ganglia and reduction of myocardial MIBG uptake in FAP.^{30,46} The concordance between the reduced SGIIPGP 9.5 and the symptom of orthostatic hypotension in the present study indicates the synchronous degeneration of sympathetic cholinergic and norepinephrinergic nerves.

The PGP 9.5⁺ sudomotor innervation was intriguingly associated with the ambulation status at the time of skin biopsy and the further progression of disability in addition to the CMAP amplitude of peroneal nerves. Such a pattern of clinical correlation indicates that the sudomotor innervation may reflect the global status of nerve functions and potentially serves as a prognostic marker for the evolution of neurological disability in FAP. In the past, only limited tools could provide prognostic predictions for the long-term progression of FAP, for example, using MIBG imaging on the Val30Met variant to show the association of lower late heart-to-mediastinum MIBG uptake ratio with a higher 5-year mortality rate.²⁹ The present study highlights the potential of applying pathologic assessment of sudomotor innervation by skin biopsies as a prognostic factor for the current disability and progression in FAP. The association between the SGIIPGP 9.5 and the progression of neurological disability suggest that sudomotor denervation may reflect the underlying gross nerve degeneration.

In contrast to SGIIPGP 9.5, there was no correlation between SGIIVIP and clinical parameters. This finding suggests the structural degeneration (PGP 9.5) instead of decreased neuropeptide expression (VIP) in sudomotor nerves reflects the clinical manifestations. An alternative explanation underlying such a lack of correlation is the marked reduction of VIP⁺ nerves in FAP. The percentile rank of SGIIVIP according to the normative data was below the 1st percentile in most FAP patients. This distribution of SGIIVIP at the markedly low level might lessen the statistical strength of correlations with clinical parameters.

The present study demonstrates the pathology and its clinical significance of sudomotor denervation in the TTR missense mutation Ala97Ser-related FAP, a late onset generalized disabling neuropathy. Given that skin biopsies were performed at a mean time of 2.3 years after the symptom onset, this suggests that sudomotor nerve degeneration had developed at an early stage of symptomatic FAP. Once neuropathic symptoms began, patients lost ambulation ability within 2 to 8 years. In the present series of patients, autonomic dysfunction was the initial symptom in 7.1% of the patients, and 78.6% of patients had autonomic dysfunctions at the time of skin biopsy, suggesting common involvement of autonomic nerves during disease progression. Given that FAP is

characterized by early and selective involvement of small-fiber nerves,^{26,47} our findings suggest that skin biopsy can provide pathological evidence for small-fiber nerve degeneration including both thermal–nociceptive sensory and sudomotor autonomic nerves, and can serve as a potential tool for early detection of FAP, for example, by the future application of skin biopsy with IENF and SGII evaluations to asymptomatic carriers of FAP.²⁶

Acknowledgment

This work was supported by grants from the National Science Council, Taiwan (101-2314-B-002-163-MY3, 102-2321-B-002-082-, C.-C.C.; 100-2320-B-002-083-MY3, 102-2321-B-002-061, S.-T.H.) and Translational Medicine Project of National Taiwan University College of Medicine and National Taiwan University Hospital (101C101-201, S.-T.H.).

Authorship

C.-M.H., H.-H.C., K.-R.L., H.-W.K. contributed equally to this work.

Potential Conflicts of Interest

Nothing to report.

References

1. Plante-Bordeneuve V, Said G. Familial amyloid polyneuropathy. *Lancet Neurol* 2011;10:1086–1097.
2. Ando Y, Nakamura M, Araki S. Transthyretin-related familial amyloidotic polyneuropathy. *Arch Neurol* 2005;62:1057–1062.
3. Ikeda S, Nakazato M, Ando Y, Sobue G. Familial transthyretin-type amyloid polyneuropathy in Japan: clinical and genetic heterogeneity. *Neurology* 2002;58:1001–1007.
4. Yang NC, Lee MJ, Chao CC, et al. Clinical presentations and skin denervation in amyloid neuropathy due to transthyretin Ala97ser. *Neurology* 2010;75:532–538.
5. Freeman R. Autonomic peripheral neuropathy. *Lancet* 2005;365:1259–1270.
6. Luo KR, Chao CC, Chen YT, et al. Quantitation of sudomotor innervation in skin biopsies of patients with diabetic neuropathy. *J Neuropathol Exp Neurol* 2011;70:930–938.
7. Gibbons CH, Illigens BM, Wang N, Freeman R. Quantification of sweat gland innervation: a clinical-pathologic correlation. *Neurology* 2009;72:1479–1486.
8. Liu Y, Billiet J, Ebenezer GJ, et al. Factors influencing sweat gland innervation in diabetes. *Neurology* 2015;84:1652–1659.
9. Luo KR, Chao CC, Hsieh PC, et al. Effect of glycemic control on sudomotor denervation in type 2 diabetes. *Diabetes Care* 2012;35:612–616.
10. Vaalasti A, Tainio H, Rechart L. Vasoactive intestinal polypeptide (VIP)-like immunoreactivity in the nerves of human axillary sweat glands. *J Invest Dermatol* 1985;85:246–248.

11. Suhr OB, Holmgren G, Steen L, et al. Liver transplantation in familial amyloidotic polyneuropathy. Follow-up of the first 20 Swedish patients. *Transplantation* 1995;60:933–938.
12. Chao CC, Tsai LK, Chiou YH, et al. Peripheral nerve disease in SARS: report of a case. *Neurology* 2003;61:1820–1821.
13. Chao CC, Hsieh SC, Yang WS, et al. Glycemic control is related to the severity of impaired thermal sensations in type 2 diabetes. *Diabetes Metab Res Rev* 2007;23:612–620.
14. Yarnitsky D, Ochoa JL. Warm and cold specific somatosensory systems. Psychophysical thresholds, reaction times and peripheral conduction velocities. *Brain* 1991;114:1819–1826.
15. Ravits JM. AAEM minimonograph #48: Autonomic nervous system testing. *Muscle Nerve* 1997;20:919–937.
16. McCarthy BG, Hsieh ST, Stocks A, et al. Cutaneous innervation in sensory neuropathies: evaluation by skin biopsy. *Neurology* 1995;45:1848–1855.
17. Chien HF, Tseng TJ, Lin WM, et al. Quantitative pathology of cutaneous nerve terminal degeneration in the human skin. *Acta Neuropathol* 2001;102:455–461.
18. Shun CT, Chang YC, Wu HP, et al. Skin denervation in type 2 diabetes: correlations with diabetic duration and functional impairments. *Brain* 2004;127:1593–1605.
19. Howie AJ, Brewer DB, Howell D, Jones AP. Physical basis of colors seen in Congo red-stained amyloid in polarized light. *Lab Invest* 2008;88:232–242.
20. Khurana R, Uversky VN, Nielsen L, Fink AL. Is Congo red an amyloid-specific dye? *J Biol Chem* 2001;276:22715–22721.
21. Prakash R, Bharathi Raja S, Devaraj H, Devaraj SN. Up-regulation of Muc2 and Il-1beta expression in human colonic epithelial cells by Shigella and its interaction with mucins. *PLoS One* 2011;6:e27046.
22. Howie AJ, Brewer DB. Optical properties of amyloid stained by Congo red: history and mechanisms. *Micron* 2009;40:285–301.
23. Pan CL, Tseng TJ, Lin YH, et al. Cutaneous innervation in Guillain-Barre syndrome: pathology and clinical correlations. *Brain* 2003;126:386–397.
24. Nejsum LN, Praetorius J, Nielsen S. Nkcc1 and Nhe1 are abundantly expressed in the basolateral plasma membrane of secretory coil cells in rat, mouse, and human sweat glands. *Am J Physiol Cell Physiol* 2005;289:C333–C340.
25. Montagna P, Salvi F, Liguori R. Sympathetic skin response in familial amyloid polyneuropathy. *Muscle Nerve* 1988;11:183–184.
26. Conceicao I, Costa J, Castro J, de Carvalho M. Neurophysiological techniques to detect early small-fiber dysfunction in transthyretin amyloid polyneuropathy. *Muscle Nerve* 2014;49:181–186.
27. Ando Y, Araki S, Shimoda O, Kano T. Role of autonomic nerve functions in patients with familial amyloidotic polyneuropathy as analyzed by laser Doppler flowmetry, capsule hydrograph, and cardiographic R-R interval. *Muscle Nerve* 1992;15:507–512.
28. Tanaka M, Hongo M, Kinoshita O, et al. Iodine-123 metaiodobenzylguanidine scintigraphic assessment of myocardial sympathetic innervation in patients with familial amyloid polyneuropathy. *J Am Coll Cardiol* 1997;29:168–174.
29. Coutinho MC, Cortez-Dias N, Cantinho G, et al. Reduced myocardial 123-iodine metaiodobenzylguanidine uptake: a prognostic marker in familial amyloid polyneuropathy. *Circ Cardiovasc Imaging* 2013;6:627–636.
30. Koike H, Misu K, Sugiura M, et al. Pathology of early- vs late-onset Ttr Met30 familial amyloid polyneuropathy. *Neurology* 2004;63:129–138.
31. Wilkinson KD, Lee KM, Deshpande S, et al. The neuron-specific protein Pgp 9.5 is a ubiquitin carboxyl-terminal hydrolase. *Science* 1989;246:670–673.
32. Landis SC, Fredieu JR. Coexistence of calcitonin gene-related peptide and vasoactive intestinal peptide in cholinergic sympathetic innervation of rat sweat glands. *Brain Res* 1986;377:177–181.
33. Tanaka E, Uchiyama S, Nakano S. Effects of calcitonin gene-related peptide and vasoactive intestinal peptide on nicotine-induced sweating in man. *J Auton Nerv Syst* 1990;30:265–268.
34. Levy DM, Terenghi G, Gu XH, et al. Immunohistochemical measurements of nerves and neuropeptides in diabetic skin: relationship to tests of neurological function. *Diabetologia* 1992;35:889–897.
35. Verdu E, Vilches JJ, Rodriguez FJ, et al. Physiological and immunohistochemical characterization of cisplatin-induced neuropathy in mice. *Muscle Nerve* 1999;22:329–340.
36. Holzbaur EL, Scherer SS. Microtubules, axonal transport, and neuropathy. *N Engl J Med* 2011;365:2330–2332.
37. Coelho T, Adams D, Silva A, et al. Safety and efficacy of RNAi therapy for transthyretin amyloidosis. *N Engl J Med* 2013;369:819–829.
38. Coelho T, Maia LF, Martins da Silva A, et al. Tafamidis for transthyretin familial amyloid polyneuropathy: a randomized, controlled trial. *Neurology* 2012;79:785–792.
39. Berk JL, Suhr OB, Obici L, et al. Repurposing diflunisal for familial amyloid polyneuropathy: a randomized clinical trial. *JAMA* 2013;310:2658–2667.
40. Provitera V, Nolano M, Caporaso G, et al. Evaluation of sudomotor function in diabetes using the dynamic sweat test. *Neurology* 2010;74:50–56.
41. Gibbons CH, Illigens BM, Centi J, Freeman R. QDIRT: quantitative direct and indirect test of sudomotor function. *Neurology* 2008;70:2299–2304.
42. Novak V, Freimer ML, Kissel JT, et al. Autonomic impairment in painful neuropathy. *Neurology* 2001;56:861–868.
43. Obayashi K, Ando Y. Focus on autonomic dysfunction in familial amyloidotic polyneuropathy (FAP). *Amyloid* 2012;19(suppl 1):28–29.
44. Freeman R. Clinical practice. neurogenic orthostatic hypotension. *N Engl J Med* 2008;358:615–624.
45. Suzuki T, Higa S, Sakoda S, et al. Orthostatic hypotension in familial amyloid polyneuropathy: treatment with DL-threo-3,4-dihydroxyphenylserine. *Neurology* 1981;31:1323–1326.
46. Delahaye N, Dinanian S, Slama MS, et al. Cardiac sympathetic denervation in familial amyloid polyneuropathy assessed by iodine-123 metaiodobenzylguanidine scintigraphy and heart rate variability. *Eur J Nucl Med* 1999;26:416–424.
47. Said G, Ropert A, Faux N. Length-dependent degeneration of fibers in Portuguese amyloid polyneuropathy: a clinicopathologic study. *Neurology* 1984;34:1025–1032.